ISSN 0915-633X

NATIONAL INSTITUTE FOR FUSION SCIENCE

Fast Cooling Phenomena with Ice Pellet Injection in the JIPP T-IIU Tokamak

M. Sakamoto, K. N. Sato, Y. Ogawa, K. Kawahata
S. Hirokura, S. Okajima, K. Adati, Y. Hamada
S. Hidekuma, K. Ida, Y. Kawasumi, M. Kojima
K. Masai, S. Morita, H. Takahashi
Y. Taniguchi, K. Toi and T. Tsuzuki

(Received – Oct. 7, 1991)

NIFS-116 Oct. 1991

RESEARCH REPORT
NIFS Series

NAGOYA, JAPAN

Fast Cooling Phenomena with Ice Pellet Injection in the JIPP T-IIU Tokamak

M.SAKAMOTO, K.N.SATO, Y.OGAWA, K.KAWAHATA, S.HIROKURA, S.OKAJIMA*, K.ADATI, Y.HAMADA, S.HIDEKUMA, K.IDA, Y.KAWASUMI, M.KOJIMA, K.MASAI, S.MORITA, H.TAKAHASHI, Y.TANIGUCHI, K.TOI and T.TSUZUKI

National Institute for Fusion Science, Nagoya 464-01, Japan

*Faculity of Engineering, Chubu University, Kasugai 487, Japan

Abstract

Ice pellet injection experiments were carried out in the JIPP T-IIU tokamak in order to study thermal (cooling) transport just after injection. The cut-off problem of ECE signals due to the rise in density has been resolved by careful measurements of temperature profile at a high time resolution (Δt=2ms) during its decay phase. The phenomenon of ultra-fast cooling (so-called pre-cooling) has been identified using the two different methods of ECE and soft X-ray(SXR) measurements. In the outer region ($r>r_{inv}$) of the plasma the cooling propagation velocity is comparable to or slightly greater than the pellet velocity, while in the central region ($r<r_{inv}$) the propagation velocity is significantly greater than the pellet velocity. Ice pellet were injected into various kinds of JIPP T-IIU plasmas, the current and sawtooth phase of which had different values, including a no-sawtooth plasma. The existence of the sawtooth oscillation and arrival of a pellet near the inversion radius r_{inv} of the sawtooth oscillations have turned out to be necessary conditions for the pre-cooling, and even just after the sawtooth crash the pre-cooling may start around the q=1 surface, not at the plasma center. Simultaneous measurements of electron temperature and density profiles indicate that the central temperature always decreases before the central density increases. Some anomalous transport might be induced by pellet injection at the central region.

Keywords ; JIPP T-IIU tokamak, ice pellet injection, cooling transport, sawtooth oscillation, q=1 surface

1. Introduction

Ice pellet injection is indispensable for fueling magnetic fusion reactors. Many important characteristics of plasmas have been observed with pellet injection experiments. In Alcator-C (GREENWALD et al., 1984) the global energy confinement time of a pellet-fueled Ohmic plasma increased with increasing electron density in the high-density range. In JT-60 (KAMADA et al.,1989), the enhanced energy confinement was observed when a pellet reached inside the q=1 surface. Improved confinement modes have been observed in Doublet-III (SENGOKU et al., 1985) and ASDEX plasmas (KAUFMANN et al., 1988). Associated with the peaked density profile due to pellet fueling are the temporal behavior just after the pellet injection, which has given fruitful informations about particle transport, and the particle diffusion coefficient and inward pinch velocity, which have been analyzed in some devices [ASDEX (VLASES et al.,1987), TFTR (HULSE et al.,1987) and JIPP T-IIU (KAWAHATA et al., 1989a)]. Related to the MHD activity are snake oscillations at the q=1 surface, which have been observed in JET plasmas (WELLER et al., 1987). Ice pellet injection is also useful as a plasma diagnostics, e.g., the safety factor has been measured in TEXT (DURST et al.,1988).

The so-called pre-cooling phenomenon (ultra-fast propagation of the cooling front) is another interesting characteristic of torus plasmas, where the speed of propagation of the cooling front due to pellet injection is much faster than the speed of the injected pellet, as observed in ASDEX (VLASES et al., 1983),

Alcator-C (GREENWALD et al., 1985), TFR (EQUIPE TFR, 1985, 1987), JET (CHEETHAM et al., 1987), and Doublet-III (SCHISSEL et al., 1987). In TFR, the speed of propagation of the cooling front increases monotonically from the edge of the plasma to the q=1 surface and increases drastically inside the q=1 surface. In JET, outside the sawtooth inversion radius there is no evidence of the cooling front propagating faster than the pellet speed, but the electron temperature over the whole central region decreases immediately when the pellet reaches the sawtooth inversion radius. However, it has been considered that the results from the ECE diagnostics might not be real phenomena because of the cut-off problem of ECE signals due to the quick increase in density.

The pre-cooling phenomenon has also been observed in JIPP T-IIU plasmas (SAKAMOTO et al., 1990). In order to study phenomenon in more detail, and especially to examine the cut-off problem, time- and space-resolved diagnostics (ECE, soft X-ray and interferometer) were utilized and time evolutions of both the electron temperature and density profiles were simultaneously measured. In particular, the cut-off of ECE signals due to a large increase in density with pellet injection has been carefully avoided by measuring the electron temperature profile over the whole region of the plasma column and by comparing this with the soft X-ray signals. This paper presents our experimental studies on the pre-cooling phenomenon with ice pellet injection, and particularly the correlation with sawtooth activity. In addition, simultaneous measurements of electron temperature and density profiles have made it possible to suggest the mechanism behind the fast cooling phenomenon.

The experimental set-up and diagnostics system for this study are presented in Section 2. In Section 3, the experimental results are described and discussed,and the conclusions are given in Section 4.

2. Experimental Set-up and Diagnostics

In the JIPP T-IIU tokamak (R/a=0.91m/0.23m, circular cross-section, B_T=3T), ice pellet injection experiments were carried out with gas-gun-type single-pellet injectors, the pellet size of which is 1.4mmΦ x 1.4mmL or 1.0mmΦ x 1.0mmL. The velocity of the pellet is in the range of 400-900 m/s, which is routinely measured by a time-of-flight technique with two optical sets.

The layout of the device and diagnostics system is shown in Fig.1. The electron temperature was measured by electron cyclotron emission (ECE) signals with a 10-channel grating polychromator (KAWAHATA et al., 1988), the temporal and spatial resolutions of which are Δt=2ms and Δr=2cm, respectively. The electron density profile was measured with a 6-channel far-infrared (HCN laser ; λ=337μm) interferometer (Δt=200ms , Δr=2cm) (KAWAHATA et al., 1989b). Soft X-ray emission from the plasma was measured with an 8 channel detector array of Si surface-barrier diodes (Δt=2ms, Δr=1.5cm), with an energy range 0.8-20keV. The trajectories of the pellets were observed tangentially with a CCD camera, as shown in Fig.1.

3. Experimental Results and Discussion

The time evolution of typical plasma parameters with ice pellet injection is shown in Fig.2. The plasma current was 210 kA, the line- averaged electron density n_e was 5.6×10^{19} m^{-3}, and the central electron temperature $T_e(0)$ was 1.1 keV for the target plasma. Just after pellet injection, the density increased to $n_e = 9.3 \times 10^{19} m^{-3}$ and the electron temperature decreased to 0.57 keV. The loop voltage had a positive spike due to the decrease in temperature, while the plasma current was kept constant. The decay in the density once raised by pellet injection was remarkably slower than the recovery in the electron temperature. The energy stored in the plasma gradually increased with a time constant of about 15 ms, and this is almost consistent with the density and temperature behaviors.

3-1. Pre-cooling phenomenon

Figure 3 shows the time evolution of the electron temperature measured by the ECE system at 10 different major radii at ice pellet injection. The major radius R_0 of the center of the plasma was about 88.0 cm, and the ECE signals covered almost the whole region of the plasma column (i.e., $-0.5 < r/a < 0.92$, $r=R-R_0$). Since the inversion radius r_{inv} of the sawtooth oscillations was about 6 cm, the major radii 84.3, 88.3 and 92.2 cm were inside r_{inv}. In this discharge, the pellet injected from the outer midplane is proved to have penetrated up to R=91.5 cm by measurement from a CCD camera.

In the case of pellet-injected plasmas, it is always

important to examine the validity of the ECE signals due to the cut-off problem caused by the sharp rise in density. Although the pellet was injected from the low-field side, the signals from the high-field side begin to decrease almost simultaneously with those from the low-field side, as shown in Fig.3. Hence the experimentally-observed profile of the electron temperature decays almost symmetrically, as expected from the fast relaxation along the magnetic field lines (τ_{ee}~10ms). This symmetrical decay of the temperature profile indicates that the ECE signals are free from the cut-off problem caused by the rise in density. If there is a cut-off layer in a plasma, it should result in a big dip in the measured "temperature profile" of the low-field side and thus the profile should become asymmetrical, as pointed out by CAMPBELL and EBERHAGEN (1984). Actually, such a dip in the "temperature profile" on the low-field side was also measured when a large pellet was injected into a high-density plasma.

The cooling front (the start of the temperature drop at each radius) is indicated by arrows in Fig.3. The start of the drop in temperature has been defined as a 20 % decrease of the temperature change ΔT_e due to pellet injection, in order to remove the ambiguity caused by the fluctuation of the signals. Figure 4 represents the position of the cooling front, denoted by arrows in Fig.3, as a function of its arrival time. The position of the sawtooth inversion and the ablation region (penetration depth) as measured by a CCD camera are also shown in the figure. In this case, the pellet was injected inside the sawtooth inversion radius. It has been found that the propagation velocity of the cooling front is not constant in the plasma

column. In the outer region of the plasma column, the cooling front penetrates into the plasma with a moderate and constant speed. The upper solid line in Fig.4 was drawn by the least-squares method of four points for major radii larger than 95 cm. The velocity obtained from the gradient of the solid line is 690 m/s, which is comparable with the velocity of the pellet. The lower line was drawn to be symmetrical to the upper line with respect to the plasma center. The observational data from the high-field side (R<82cm) roughly coincide with the lower line, and this implies that the cooling front propagates concentrically from the edge to the central region of the plasma, accompanied by quick relaxation along the magnetic surface. The propagation velocities of the cooling front in the outer region in all cases are in the range of about 700-1600m/s, which is comparable to or slightly faster than the pellet velocities (400-900m/s). Since the propagation velocity is systematically larger within a factor of one to two than the injected pellet speed, some pre-cooling mechanism might exist even in the outer region.

On the other hand, the propagation velocity in the central region is significantly faster than the pellet velocity. Roughly speaking, this pre-cooling speed is one or more orders of magnitude faster than the pellet speed, although the scattering of the data is large.

This feature has also been supported by chord-integrated soft X-ray measurements. As shown in Fig.5, the SXR signals have decayed due to pellet injection. The time at which each soft X-ray signal starts to decay is shown by crosses in Fig.4. This indicates the existence of fast-cooling phenomenon, as do the ECE

measurements.

The intensity of the soft X-rays is a function of the electron temperature, density and impurity concentration. When soft X-rays are dominated by Bremsstrahlung without significant change in the impurity concentration, the change in the SXR signal ΔI is approximately related to the temperature and density changes, ΔT_e and Δn_e, by the following equation:

$$\Delta I/I \sim (1/2+\varepsilon_1/T_e)\Delta T_e/T_e + 2\Delta n_e/n_e, \qquad (1)$$

where ε_1 is the lower limit (ε_1~800eV) of the energy range for SXR measurements. In the outer region of the plasma column, where the electron temperature is lower than $2\varepsilon_1/3$, i.e. r/a>0.5, the value of ΔI / I is more sensitive to ΔT_e rather than Δn_e. The decrease in the SXR signals at the dominant ablation region(r/a~0.5), where $|\Delta T_e/T_e| = |\Delta n_e/n_e|$, may be explained by equation (1). We should take into consideration that the remarkable decrease in the SXR signals was observed at the central region of the plasma, where the rate of change $\Delta I/I$ is more sensitive to Δn_e rather than ΔT_e. This implies that the density at the central region did not increase just as the cooling front arrived at the center, which implies pre-cooling. This is confirmed by direct measurements of density and temperature profiles, which are presented in section 3-3.

3-2. Correlation between pre-cooling and sawtooth activity

Figure 4 shows that pre-cooling starts near the region of sawtooth inversion. As described in the Introduction, a strong correlation of the cooling propagation speed with the sawtooth

inversion radius has been observed in TFR and JET. In order to examine the relation between the sawtooth oscillation and pre-cooling, pellets were injected into various kinds of JIPP T-IIU plasmas, i.e. with different values of current and sawtooth phase.

The propagation of the cooling front is shown in Fig.6 in the same way as in Fig.4, where an ice pellet was injected into an Ohmically- heated plasma without sawtooth activity (a no-sawtooth plasma), where the plasma current was about 100 kA. The two solid lines in this figure were drawn by the least-squares method. It is found that the cooling front propagates from the edge to the center of the plasma with constant speed and the pre-cooling never occurred. This implies that the existence of the sawtooth oscillation is a necessary condition for pre-cooling.

Next, we examined pellet injection in the case where the pellet never reached the sawtooth inversion radius. Figure 7 shows the temporal behavior of ECE signals when the region of sawtooth inversion was around R=95cm and the pellet penetrated to R=100cm. We can see no drastic change in the ECE signals around the central region of the plasma column, although the cooling propagation velocity throughout the ablation region is comparable to the pellet velocity. Therefore, these data tell us that for pre-cooling it is necessary for the pellet to reach the sawtooth inversion radius.

The correlation between pre-cooling and sawtooth oscillation was examined in more detail. Pellets were injected into plasmas with various plasma currents. Figure 8 shows the dependence of the position r_{pre} (minor radius at the start of pre-cooling) on

the sawtooth inversion radius r_{inv}. The position r_{pre} is defined by the intersection of the extrapolation lines of the ECE signals inside and outside r_{inv}, as shown by the sketch in Fig.8. The solid line shows $r_{pre} = r_{inv}$ and it is found that r_{pre} is almost always less than r_{inv}. This indicates that pre-cooling had started to occur inside the sawtooth inversion radius.

The dependence of the pre-cooling characteristics on the sawtooth phase (0% and 100% mean just after and before the sawtooth collapse, respectively) is shown in Fig.9, where r_{pre} has been normalized by r_{inv}. A standard sawtooth model predicts that just after the sawtooth crash (i.e. the case of 0% phase), the value of q at the plasma center is almost unity. Thus, the model suggests that pre-cooling should start at the plasma center, if it is assumed to have a strong correlation with the q=1 surface. This , however, contradicts the results given in Fig.9, where the normalized radius r_{pre} has a weak dependence on the sawtooth phase and clearly has an off-set at phase 0%, although the scattering of the data is large. Another possibility that could explain these data is that the central value of q, q(0), is kept sufficiently below unity even just after the sawtooth crash, as observed experimentally in TEXTOR (SOLTWISCH , 1986) and TEXT (WEST et al., 1987). According to this model, the explanation may be that pre-cooling starts just at this q=1 surface far from the plasma center, but inside the standard sawtooth inversion radius.

3-3. Simultaneous measurements of density and temperature profiles

In this section, we discuss the mechanism of the pre-cooling. As previously stated, the time-evolution of SXR signals suggests that the central density never increased at the pre-cooling phase. This is because the SXR signals from the central region quickly decayed just after pellet injection, even though the signals should be more sensitive to the change in density than the change in temperature. We measured the density profile with a 6-channel interferometer to examine the change of central density just after injection. Figure 10(a) shows the density profiles just before and after injection. The pellet was ablated mainly at r=a/2 and the profile had become hollow. The error of the central density measurement is estimated to be $\Delta n_e(0)/n_e(0)=5\%$. The penetration depth as measured by a CCD camera was about 18 cm, which means that the pellet reached around r=5 cm. This is consistent with the change in the density profile. The temperature profiles of the plasma corresponding to this are shown in Fig.10(b). It is found that just after injection the central temperature had already decreased, although the central density had not yet changed, as suggested by the SXR data.

Next, we discuss the stored energy at pellet injection. Figure 10(c) shows the pressure profiles calculated with measured density and temperature profiles. The decrease ($-\Delta W$) and increase ($\Delta W'$) of the stored energies in the central and outer regions due to pre-cooling were calculated from Fig.10(c).

Although the difference between the pressures in the outer region before and after injection is within the error of the measurements, these two values are comparable with each other within an error of 10 %; that is, $|\Delta W-\Delta W'|/\Delta W \sim 0.1$. (here, $\Delta W \sim 60$J and this value is about 1.6 % of the total energy of the plasma.) Consequently, this may mean that the stored energy lost from the central region has been transferred to the outer region due to pre-cooling.

The mechanism behind the pre-cooling phenomenon seems difficult to predict theoretically. An explanation by GARBET et al.(1989) might be one possible candidate. Present experimental data show that the propagation time inside the sawtooth inversion radius is estimated to be a few tens of a microsecond or less and the central density never increased. In addition, a strong correlation with the sawtooth activity has been observed. Therefore, we can say that some MHD instability might play an important role in the pre-cooling phenomenon.

4. Conclusions

In the JIPP T-IIU tokamak, ice pellet injection experiments were carried out in order to study the thermal (cooling) transport in the torus plasma. The main results are summarized as follows.

(a) The phenomenon of fast cooling has been identified by two different and independent measurements, ECE and SXR. In the outer region($r>r_{inv}$) the cooling propagation velocity is comparable to or slightly faster than the

pellet velocity, while in the central region ($r<r_{inv}$) the propagation velocity is significantly faster than the pellet velocity. This is represented as "pre-cooling".

(b) Ice pellets were injected into various kinds of JIPP T-IIU plasmas, having different values of current, including a no-sawtooth plasma. As a result, it was found that the existence of the sawtooth oscillation and the arrival of a pellet near the sawtooth inversion radius are necessary conditions for pre-cooling.

(c) Pellet injection into plasmas whose sawtooth phases are different from each other indicates that there is not a strong correlation between the phase and the minor radius of the start of pre-cooling, and this relation has an off-set at the phase of 0%. This might give some information about the mechanism of sawtooth oscillation.

(d) The central temperature decreased even though the central density never increased during the pre-cooling phase.

Acknowledgments

The authors would like to thank the NBI group and the RF group for their technical support and fruitful discussions.

References

CAMPBELL D. J. and EBERHAGEN A. (1984) Plasma Phys. Controll. Fusion **26**, 689.

CHEETHAM A. D. et al. (1987) in Controlled Fusion and Plasma Physics (Proc. 14th Europ. Conf. Madrid, 1987), Vol.1, p.205.

DURST R D. et al. (1988) Rev. Sci. Instrum. **59**, 1623.

EQUIPE TFR (1985) in Plasma Physics and Controlled Nuclear Fusion Research 1984 (Proc. 10th Int. Conf. London,1984), Vol.1, p.103. IAEA, Vienna

EQUIPE TFR (1987) Nucl. Fusion **27**, 1975.

GARBET X. et al. (1989) Proc. Cadarache Workshop on Electrostatic Turbulence EUR-CEA-FC-1381, p.21.

GREENWALD M. et al. (1984) Phys. Rev. Lett. **53**, 352.

GREENWALD M. et al. (1985) in Plasma Physics and Controlled Nuclear Fusion Research 1984 (Proc. 10th Int. Conf. London,1984), Vol.1, p.45. IAEA, Vienna

HULSE et al. (1987) in Controlled Fusion and Plasma Physics (Proc. 14th Europ. Conf. Madrid, 1987), Vol.1, p.318.

KAMADA Y. et al. (1989) Nucl. Fusion **29**, 1785.

KAUFMANN M. et al. (1988) Nucl. Fusion **28**, 827.

KAWAHATA K. et al. (1988) Jpn. J. Appl. Phys. **27**, 2349.

KAWAHATA K. et al. (1989a) in Plasma Physics and Controlled Nuclear Fusion Research 1988 (Proc. 12th Int. Conf. Nice,1988), Vol.1, p.287. IAEA, Vienna

KAWAHATA K. et al. (1989) Rev. Sci. Instrum. **60**, 3734.

SAKAMOTO M. et al. (1990) in Controlled Fusion and Plasma Physics (Proc. 17th Europ. Conf. Amsterdam, 1990), Vol.1, p.227.

SCHISSEL D. P. et al. (1987) Nucl. Fusion **27**, 1063.

SENGOKU S. et al. (1985) Nucl. Fusion 25, 1475.

SOLTWISCH H. (1986) Rev. Sci. Instrum. **57**, 1939.

VLASES G. et al. (1983) in Controlled Fusion and Plasma Physics (Proc. 11th Europ. Conf. Aachen, 1983), Vol.1, p.127.

VLASES G. et.al. (1987) Nucl. Fusion **27**, 351.

WELLER A. et al. (1987) Phys. Rev. Lett. **59**, 2303.

WEST W. P. et al. (1987) Phys. Rev. Lett. **58**, 2758.

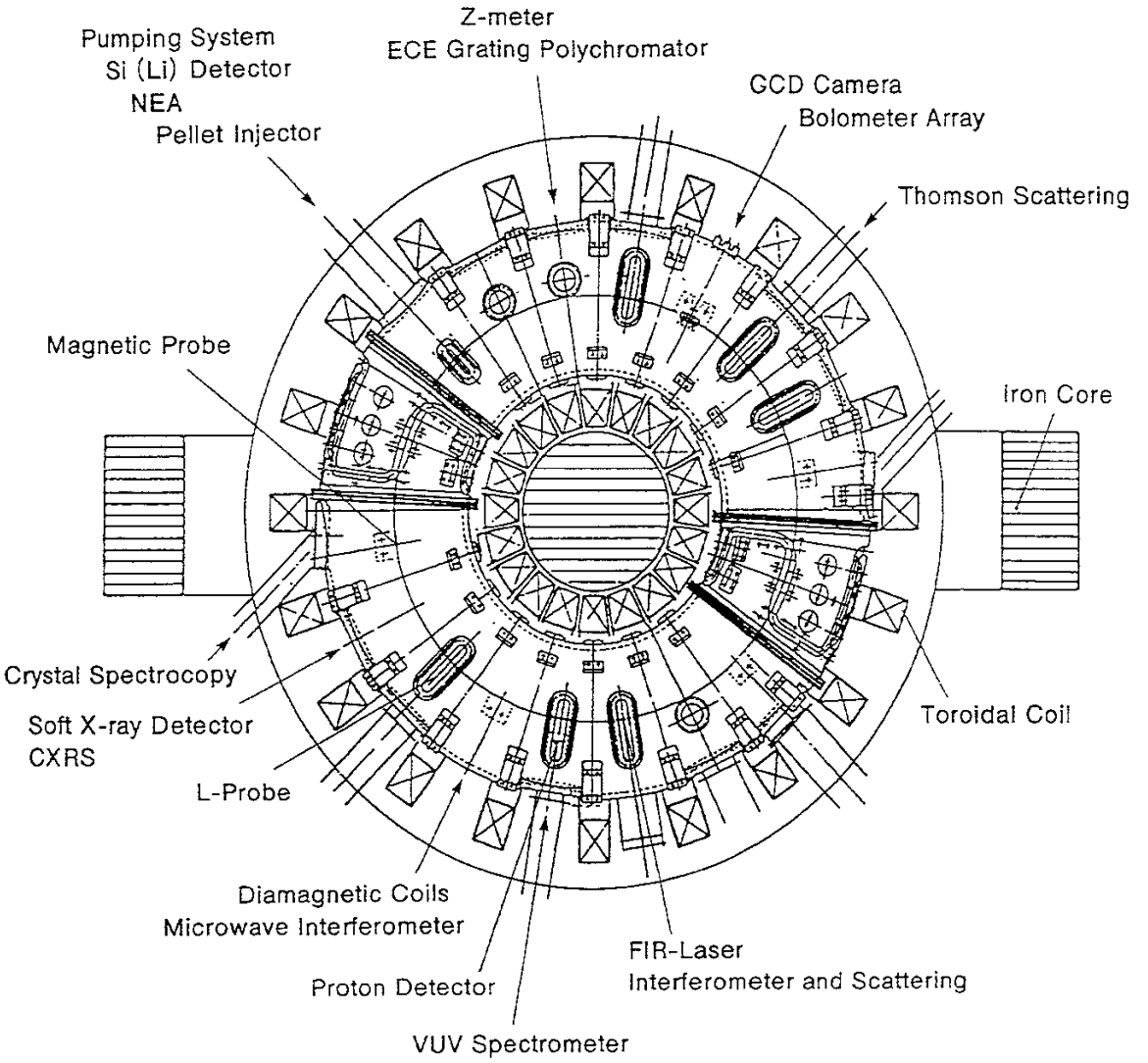

Fig. 1 Experimental arrangement of the JIPP T-IIU tokamak. The pellet injector and typical diagnostics are presented.

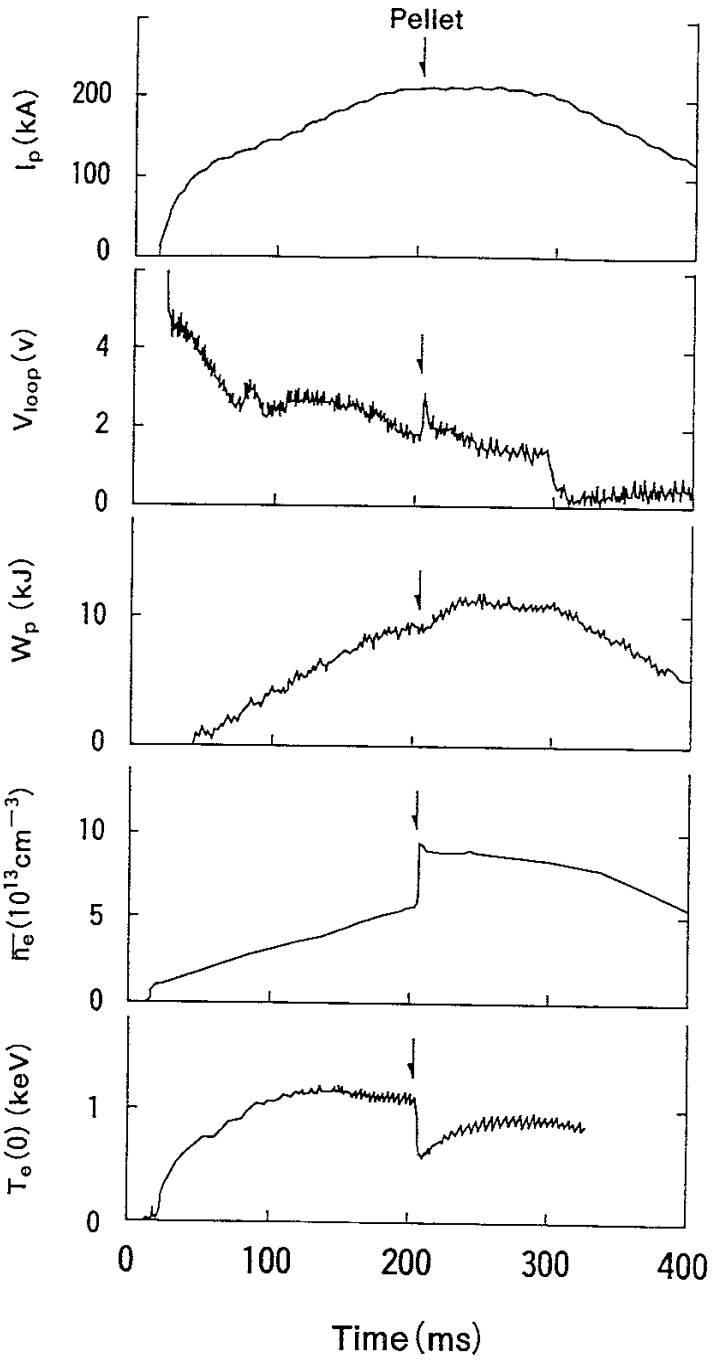

Fig. 2 Typical discharge with ice pellet injection. Shown are the plasma current I_p; one-turn voltage V_{loop}; stored energy W_p by diamagnetic measurement; line-averaged density n_e as measured by an HCN interferometer; and central electron temperature $T_e(0)$ as measured by ECE.

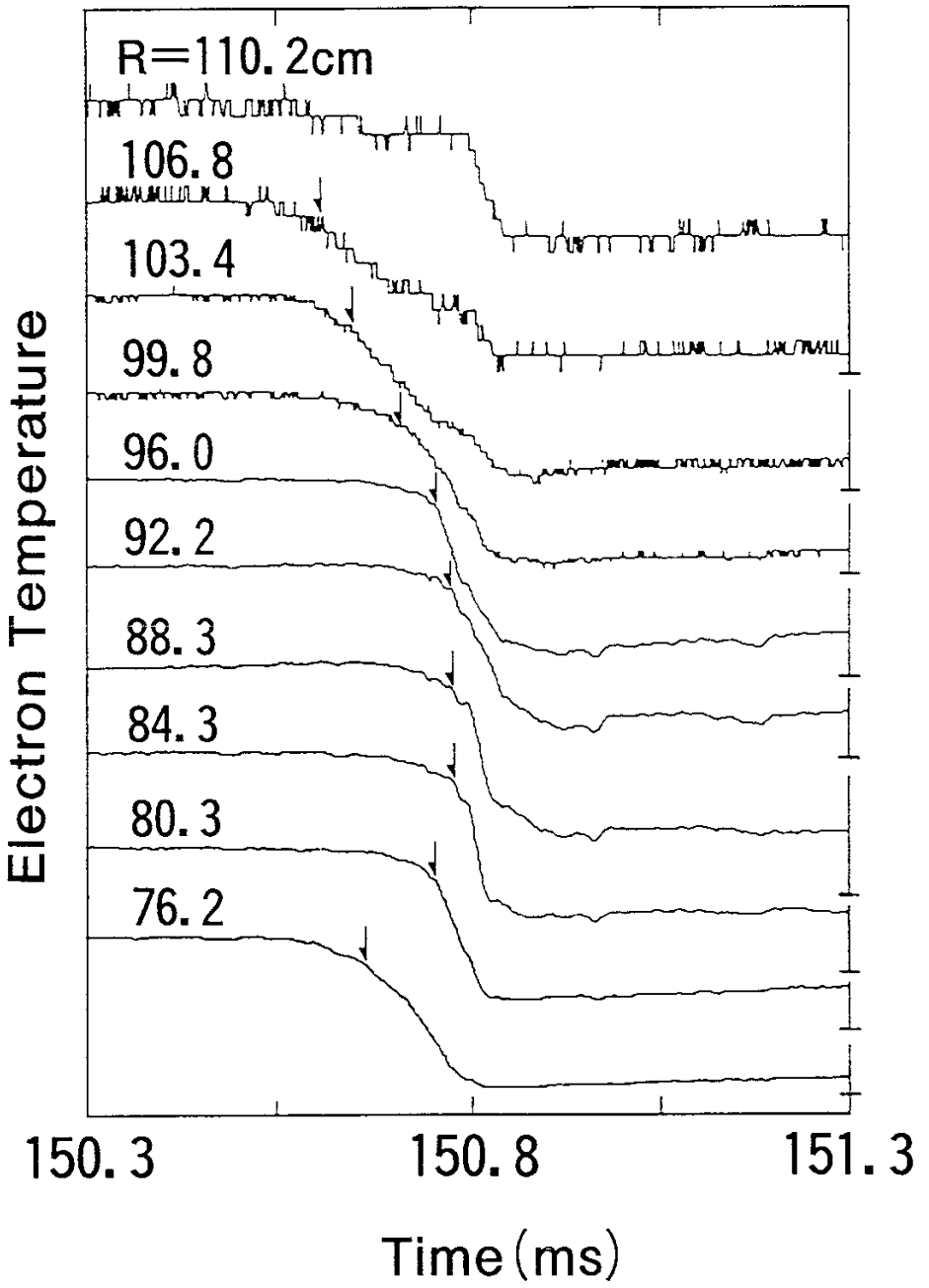

Fig. 3 Time evolution of the electron temperature with a 10-channel grating polychromator at different major radii. The pellet is injected from the low toroidal field side.

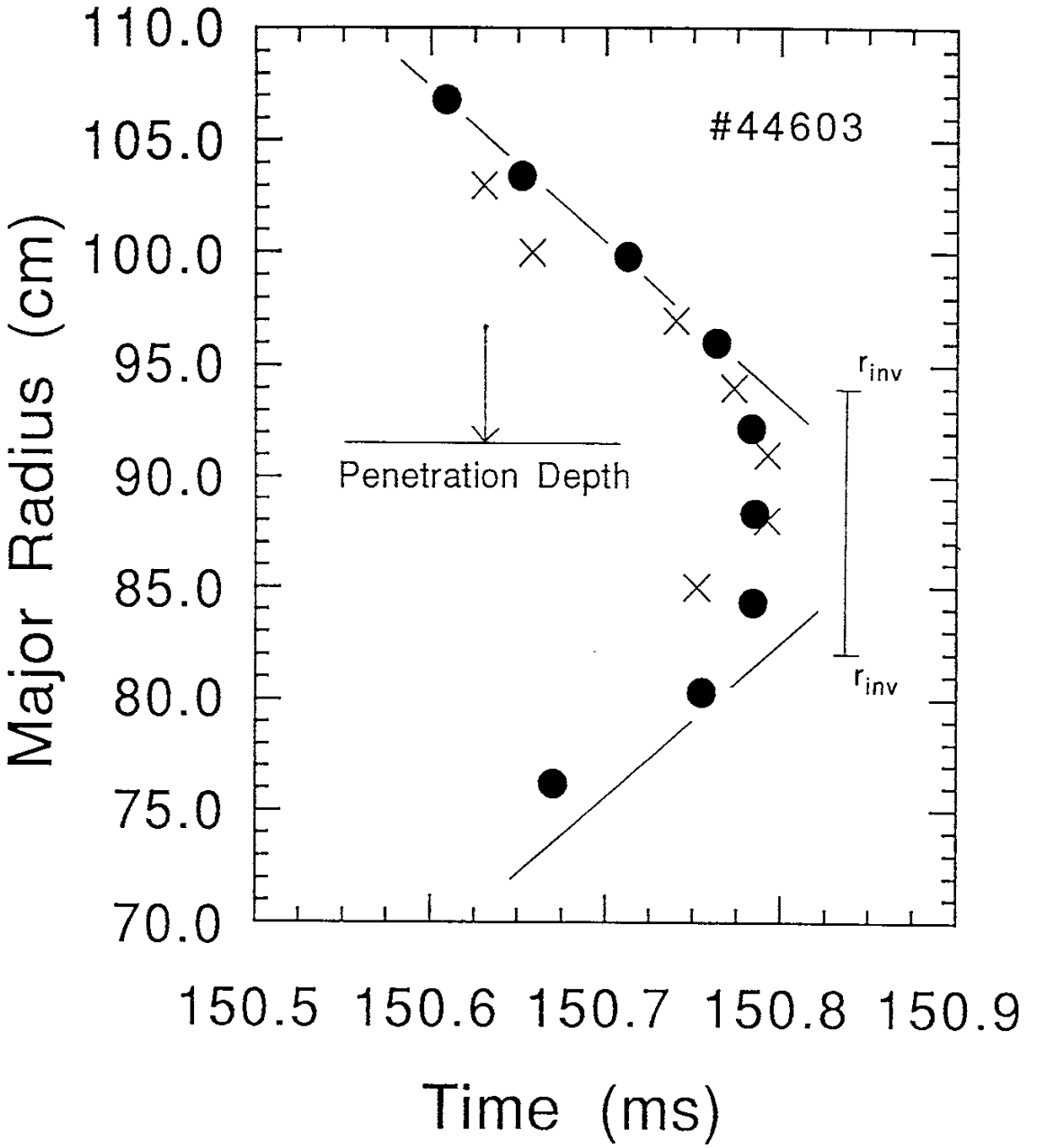

Fig. 4 Properties of the cooling front as measured by ECE (shown by arrows in Fig. 3;closed circles) and SXR (crosses).

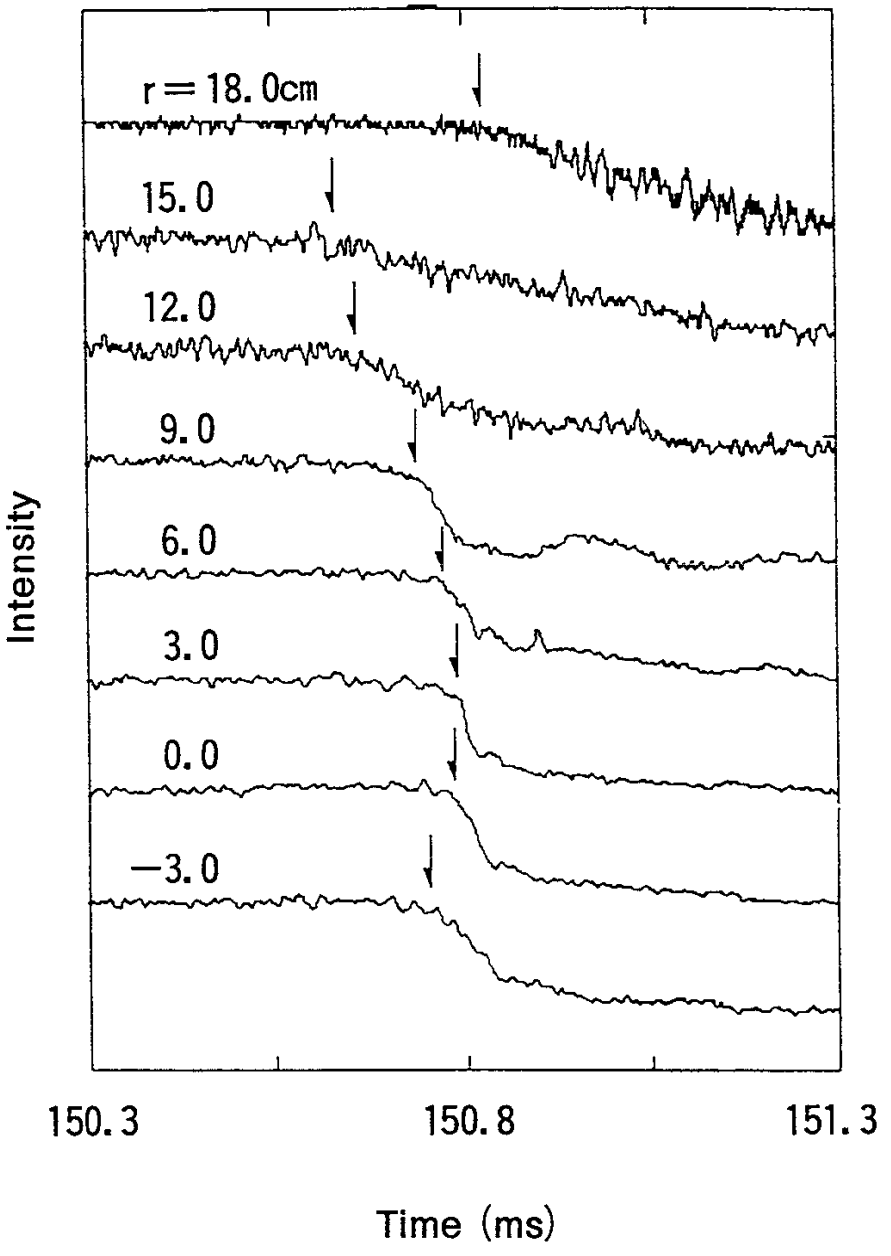

Fig. 5 Time evolution of soft X-ray signals with ice pellet injection.

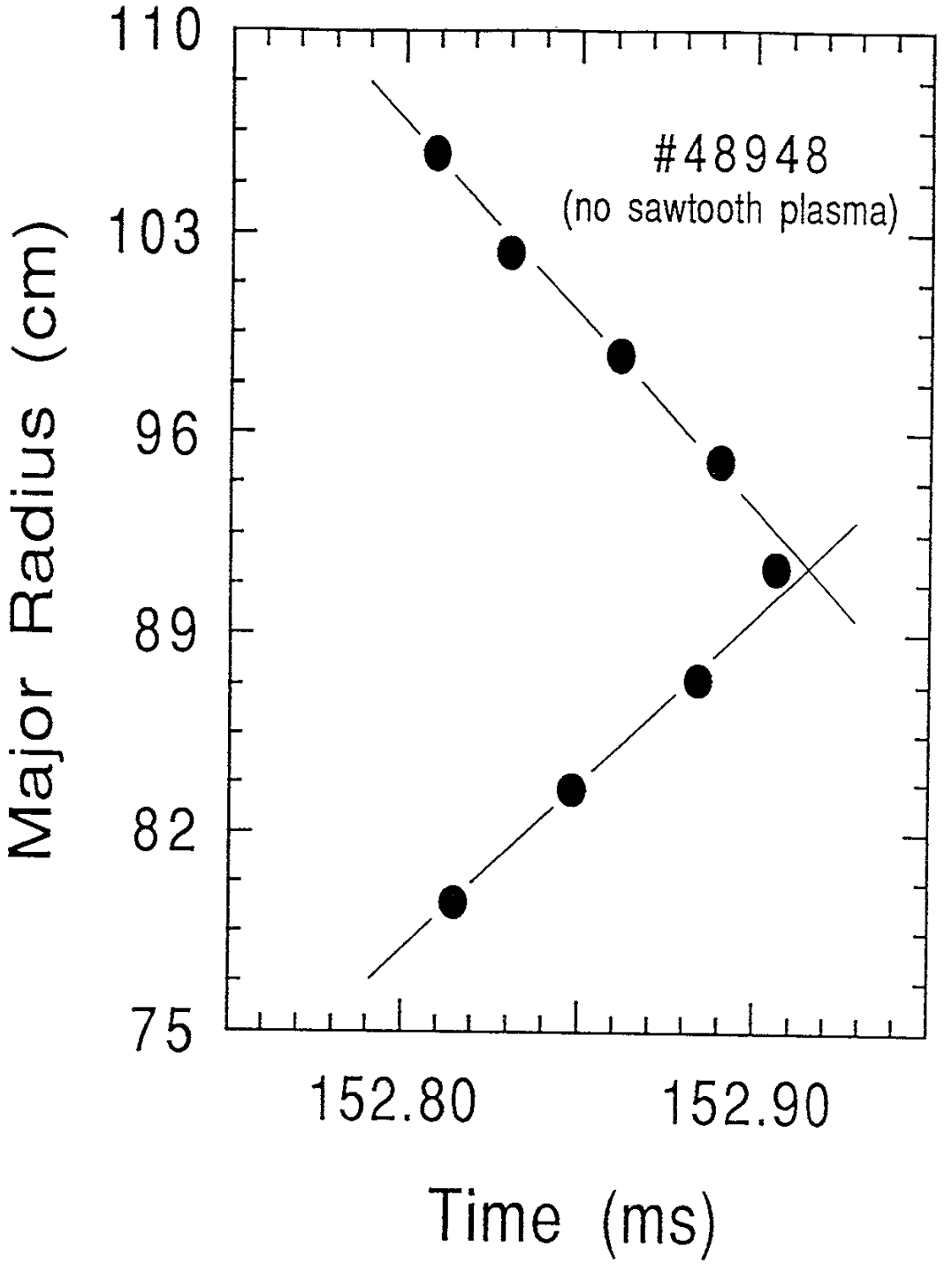

Fig. 6 Properties of the cooling front as measured by ECE when the pellet is injected into a no-sawtooth plasma.

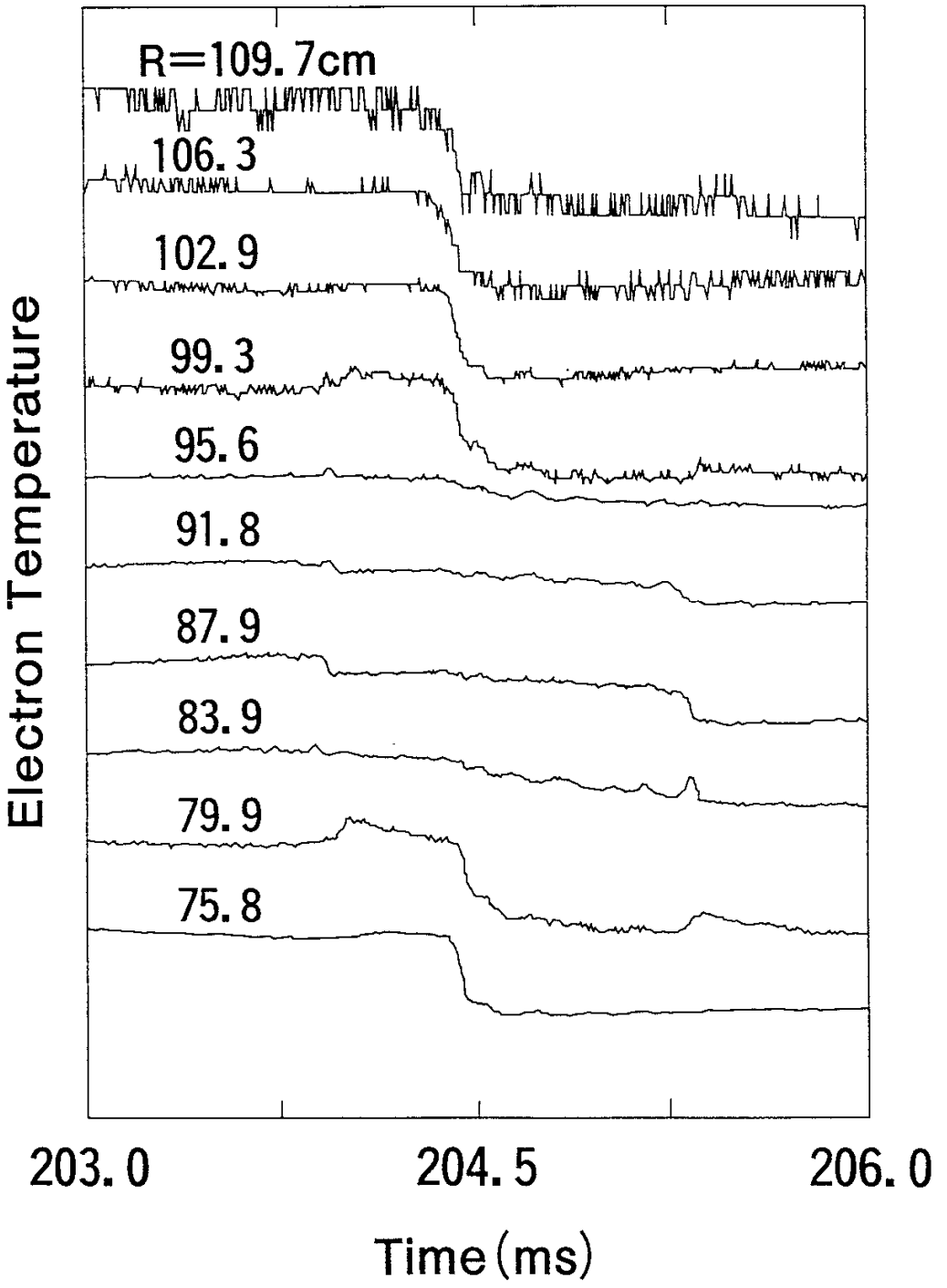

Fig. 7 Time evolution of electron temperature when the pellet does not reach the region of sawtooth inversion.

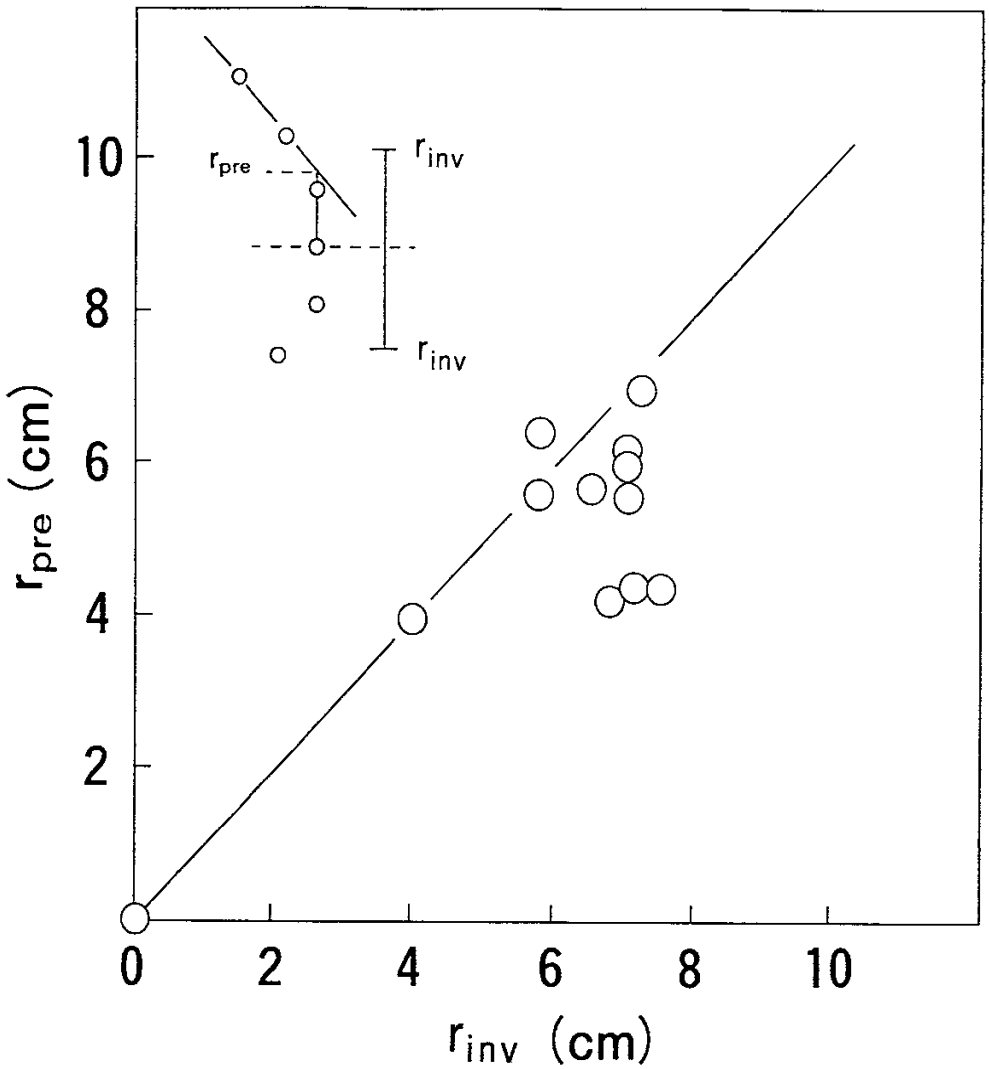

Fig. 8 Comparison of the radius at the start of pre-cooling with that of the sawtooth inversion.

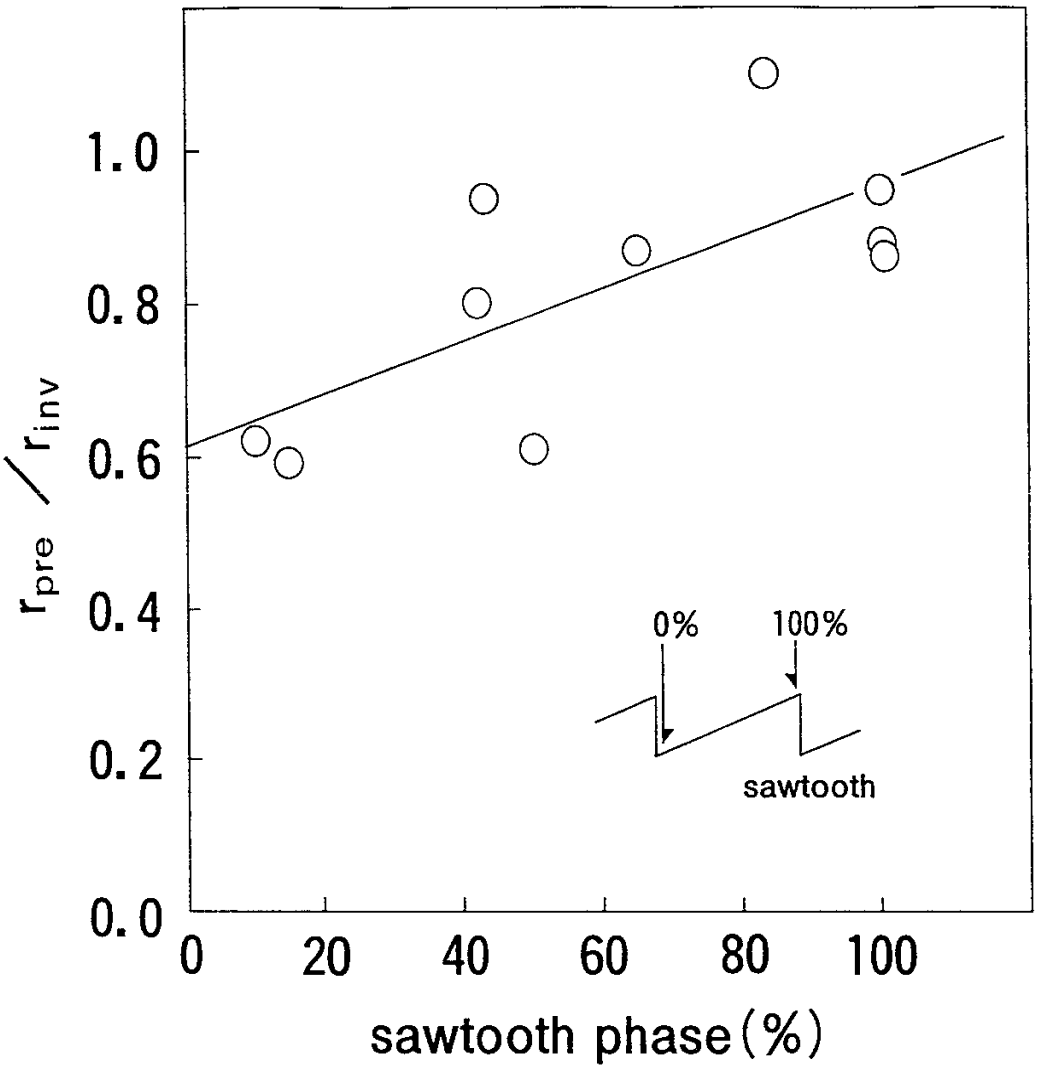

Fig. 9 Radius at the start of pre-cooling propagation, normalized by that of the sawtooth inversion as a function of sawtooth phase.

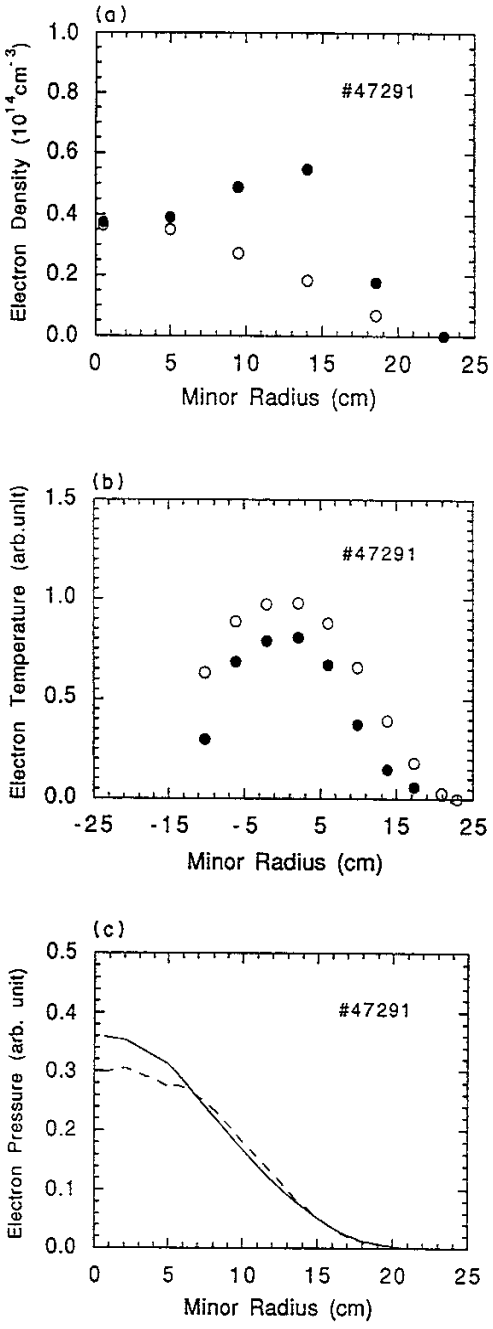

Fig. 10 (a) Electron density and (b) electron temperature profiles before (open circles) and after (closed ones) pellet injection. The electron density profile has been measured with 6-channel HCN laser interferometer. (c) Electron pressure $n_e(r)T_e(r)$ profiles calculated as the product of the measured electron density and temperature.

Recent Issues of NIFS Series

NIFS-56 H.B.Stewart and Y.Ueda, *Catastrophes with Indeterminate Outcome*; Oct. 1990

NIFS-57 S.-I.Itoh, H.Maeda and Y.Miura, *Improved Modes and the Evaluation of Confinement Improvement*; Oct. 1990

NIFS-58 H.Maeda and S.-I.Itoh, *The Significance of Medium- or Small-size Devices in Fusion Research*; Oct. 1990

NIFS-59 A.Fukuyama, S.-I.Itoh, K.Itoh, K.Hamamatsu, V.S.Chan, S.C.Chiu, R.L.Miller and T.Ohkawa, *Nonresonant Current Drive by RF Helicity Injection*; Oct. 1990

NIFS-60 K.Ida, H.Yamada, H.Iguchi, S.Hidekuma, H.Sanuki, K.Yamazaki and CHS Group, *Electric Field Profile of CHS Heliotron/Torsatron Plasma with Tangential Neutral Beam Injection*; Oct. 1990

NIFS-61 T.Yabe and H.Hoshino, *Two- and Three-Dimensional Behavior of Rayleigh-Taylor and Kelvin-Helmholz Instabilities*; Oct. 1990

NIFS-62 H.B. Stewart, *Application of Fixed Point Theory to Chaotic Attractors of Forced Oscillators;* Nov. 1990

NIFS-63 K.Konn., M.Mituhashi, Yoshi H.Ichikawa,*Soliton on Thin Vortex Filament;* Dec. 1990

NIFS-64 K.Itoh, S.-I.Itoh and A.Fukuyama,*Impact of Improved Confinement on Fusion Research;* Dec. 1990

NIFS -65 A.Fukuyama, S.-I.Itoh and K. Itoh,*A Consistency Analysis on the Tokamak Reactor Plasmas;* Dec. 1990

NIFS-66 K.Itoh, H. Sanuki, S.-I. Itoh and K. Tani,*Effect of Radial Electric Field on α-Particle Loss in Tokamaks;* Dec. 1990

NIFS-67 K.Sato,and F.Miyawaki,*Effects of a Nonuniform Open Magnetic Field on the Plasma Presheath*; Jan.1991

NIFS-68 K.Itoh and S.-I.Itoh,*On Relation between Local Transport Coefficient and Global Confinement Scaling Law;* Jan. 1991

NIFS-69 T.Kato, K.Masai, T.Fujimoto,F.Koike, E.Källne, E.S.Marmar and J.E.Rice,*He-like Spectra Through Charge Exchange Processes in Tokamak Plasmas;* Jan.1991

NIFS-70 K. Ida, H. Yamada, H. Iguchi, K. Itoh and CHS Group, *Observation of Parallel Viscosity in the CHS Heliotron/Torsatron* ; Jan.1991

NIFS-71 H. Kaneko, *Spectral Analysis of the Heliotron Field with the Toroidal Harmonic Function in a Study of the Structure of Built-in Divertor* ; Jan. 1991

NIFS-72 S. -I. Itoh, H. Sanuki and K. Itoh, *Effect of Electric Field Inhomogeneities on Drift Wave Instabilities and Anomalous Transport* ; Jan. 1991

NIFS-73 Y.Nomura, Yoshi.H.Ichikawa and W.Horton, *Stabilities of Regular Motion in the Relativistic Standard Map*; Feb. 1991

NIFS-74 T.Yamagishi, *Electrostatic Drift Mode in Toroidal Plasma with Minority Energetic Particles,* Feb. 1991

NIFS-75 T.Yamagishi, *Effect of Energetic Particle Distribution on Bounce Resonance Excitation of the Ideal Ballooning Mode*, Feb. 1991

NIFS-76 T.Hayashi, A.Tadei, N.Ohyabu and T.Sato, *Suppression of Magnetic Surface Breading by Simple Extra Coils in Finite Beta Equilibrium of Helical System;* Feb. 1991

NIFS-77 N. Ohyabu, *High Temperature Divertor Plasma Operation*; Feb. 1991

NIFS-78 K.Kusano, T. Tamano and T. Sato, *Simulation Study of Toroidal Phase-Locking Mechanism in Reversed-Field Pinch Plasma*; Feb. 1991

NIFS-79 K. Nagasaki, K. Itoh and S. -I. Itoh, *Model of Divertor Biasing and Control of Scrape-off Layer and Divertor Plasmas*; Feb. 1991

NIFS-80 K. Nagasaki and K. Itoh, *Decay Process of a Magnetic Island by Forced Reconnection*; Mar. 1991

NIFS-81 K. Takahata, N. Yanagi, T. Mito, J. Yamamoto, O.Motojima and LHDDesign Group, K. Nakamoto, S. Mizukami, K. Kitamura, Y. Wachi, H. Shinohara, K. Yamamoto, M. Shibui, T. Uchida and K. Nakayama, *Design and Fabrication of Forced-Flow Coils as R&D Program for Large Helical Device*; Mar. 1991

NIFS-82 T. Aoki and T. Yabe, *Multi-dimensional Cubic Interpolation for ICF Hydrodynamics Simulation*; Apr. 1991

NIFS-83 K. Ida, S.-I. Itoh, K. Itoh, S. Hidekuma, Y. Miura, H. Kawashima, M. Mori, T. Matsuda, N. Suzuki, H. Tamai, T.Yamauchi and JFT-2M Group, *Density Peaking in the JFT-2M Tokamak Plasma with Counter Neutral Beam Injection* ; May 1991

NIFS-84 A. Iiyoshi, *Development of the Stellarator/Heliotron Research*; May 1991

NIFS-85 Y. Okabe, M. Sasao, H. Yamaoka, M. Wada and J. Fujita, *Dependence of Au^- Production upon the Target Work Function in a Plasma-Sputter-Type Negative Ion Source;* May 1991

NIFS-86 N. Nakajima and M. Okamoto, *Geometrical Effects of the Magnetic Field on the Neoclassical Flow, Current and Rotation in General Toroidal Systems*; May 1991

NIFS-87 S. -I. Itoh, K. Itoh, A. Fukuyama, Y. Miura and JFT-2M Group, *ELMy-H mode as Limit Cycle and Chaotic Oscillations in Tokamak Plasmas;* May 1991

NIFS-88 N.Matsunami and K.Kitoh, *High Resolution Spectroscopy of H^+ Energy Loss in Thin Carbon Film;* May 1991

NIFS-89 H. Sugama, N. Nakajima and M.Wakatani, *Nonlinear Behavior of Multiple-Helicity Resistive Interchange Modes near Marginally Stable States;* May 1991

NIFS-90 H. Hojo and T.Hatori, *Radial Transport Induced by Rotating RF Fields and Breakdown of Intrinsic Ambipolarity in a Magnetic Mirror*; May 1991

NIFS-91 M. Tanaka, S. Murakami, H. Takamaru and T.Sato, *Macroscale Implicit, Electromagnetic Particle Simulation of Inhomogeneous and Magnetized Plasmas in Multi-Dimensions;* May 1991

NIFS-92 S. - I. Itoh, *H-mode Physics, -Experimental Observations and Model Theories-, Lecture Notes, Spring College on Plasma Physics, May 27 - June 21 1991 at International Centre for Theoretical Physics (IAEA UNESCO) Trieste, Italy ;* Jun. 1991

NIFS-93 Y. Miura, K. Itoh, S. - I. Itoh, T. Takizuka, H. Tamai, T. Matsuda, N. Suzuki, M. Mori, H. Maeda and O. Kardaun, *Geometric Dependence of the Scaling Law on the Energy Confinement Time in H-mode Discharges;* Jun. 1991

NIFS-94 H. Sanuki, K. Itoh, K. Ida and S. - I. Itoh, *On Radial Electric Field Structure in CHS Torsatron / Heliotron;* Jun. 1991

NIFS-95 K. Itoh, H. Sanuki and S. - I. Itoh, *Influence of Fast Ion Loss on Radial Electric Field in Wendelstein VII-A Stellarator;* Jun. 1991

NIFS-96 S. - I. Itoh, K. Itoh, A. Fukuyama, *ELMy-H mode as Limit Cycle and Chaotic Oscillations in Tokamak Plasmas;* Jun. 1991

NIFS-97 K. Itoh, S. - I. Itoh, H. Sanuki, A. Fukuyama, *An H-mode-Like Bifurcation in Core Plasma of Stellarators;* Jun. 1991

NIFS-98 H. Hojo, T. Watanabe, M. Inutake, M. Ichimura and S. Miyoshi, *Axial Pressure Profile Effects on Flute Interchange Stability in the Tandem Mirror GAMMA 10;* Jun. 1991

NIFS-99 A. Usadi, A. Kageyama, K. Watanabe and T. Sato, *A Global Simulation of the Magnetosphere with a Long Tail : Southward and Northward IMF;* Jun. 1991

NIFS-100 H. Hojo, T. Ogawa and M. Kono, *Fluid Description of Ponderomotive Force Compatible with the Kinetic One in a Warm Plasma* ; July 1991

NIFS-101 H. Momota, A. Ishida, Y. Kohzaki, G. H. Miley, S. Ohi, M. Ohnishi K. Yoshikawa, K. Sato, L. C. Steinhauer, Y. Tomita and M. Tuszewski

Conceptual Design of D-^{3}He FRC Reactor "ARTEMIS" ; July 1991

NIFS-102 N. Nakajima and M. Okamoto, *Rotations of Bulk Ions and Impurities in Non-Axisymmetric Toroidal Systems* ; July 1991

NIFS-103 A. J. Lichtenberg, K. Itoh, S. - I. Itoh and A. Fukuyama, *The Role of Stochasticity in Sawtooth Oscillation* ; Aug. 1991

NIFS-104 K. Yamazaki and T. Amano, *Plasma Transport Simulation Modeling for Helical Confinement Systems;* Aug. 1991

NIFS-105 T. Sato, T. Hayashi, K. Watanabe, R. Horiuchi, M. Tanaka, N. Sawairi and K. Kusano, *Role of Compressibility on Driven Magnetic Reconnection ;* Aug. 1991

NIFS-106 Qian Wen - Jia, Duan Yun - Bo, Wang Rong - Long and H. Narumi, *Electron Impact Excitation of Positive Ions - Partial Wave Approach in Coulomb - Eikonal Approximation* ; Sep. 1991

NIFS-107 S. Murakami and T. Sato, *Macroscale Particle Simulation of Externally Driven Magnetic Reconnection;* Sep. 1991

NIFS-108 Y. Ogawa, T. Amano, N. Nakajima, Y. Ohyabu, K. Yamazaki, S. P. Hirshman, W. I. van Rij and K. C. Shaing, *Neoclassical Transport Analysis in the Banana Regime on Large Helical Device (LHD) with the DKES Code;* Sep. 1991

NIFS-109 Y. Kondoh, *Thought Analysis on Relaxation and General Principle to Find Relaxed State;* Sep. 1991

NIFS-110 H. Yamada, K. Ida, H. Iguchi, K. Hanatani, S. Morita, O. Kaneko, H. C. Howe, S. P. Hirshman, D. K. Lee, H. Arimoto, M. Hosokawa, H. Idei, S. Kubo, K. Matsuoka, K. Nishimura, S. Okamura, Y. Takeiri, Y. Takita and C. Takahashi, *Shafranov Shift in Low-Aspect-Ratio Heliotron / Torsatron CHS* ; Sep 1991

NIFS-111 R. Horiuchi, M. Uchida and T. Sato, *Simulation Study of Stepwise Relaxation in a Spheromak Plasma ;* Oct. 1991

NIFS-112 M. Sasao, Y. Okabe, A. Fujisawa, H. Iguchi, J. Fujita, H. Yamaoka and M. Wada, *Development of Negative Heavy Ion Sources for Plasma Potential Measurement* ; Oct. 1991

NIFS-113 S. Kawata and H. Nakashima, *Tritium Content of a DT Pellet in Inertial Confinement Fusion* ; Oct. 1991

NIFS-114 M. Okamoto, N. Nakajima and H. Sugama, *Plasma Parameter Estimations for the Large Helical Device Based on the Gyro-Reduced Bohm Scaling* ; Oct. 1991

NIFS-115 Y. Okabe, *Study of Au^- Production in a Plasma-Sputter Type Negative Ion Source* ; Oct. 1991